Forecasting climate change impacts on plant populations over large spatial extents

Andrew T. Tredennick[*1], Mevin B. Hooten[2,3,4], Cameron L. Aldridge[5], Collin G. Homer[6], Andrew R. Kleinhesselink[1], and Peter B. Adler[1]

[1]*Department of Wildland Resources and the Ecology Center, 5230 Old Main Hill, Utah State University, Logan, Utah 84322 USA*

[2]*U.S. Geological Survey, Colorado Cooperative Fish and Wildlife Research Unit, Colorado State University, Fort Collins, CO 80523 USA*

[3]*Department of Fish, Wildlife, and Conservation Biology, Colorado State University, Fort Collins, CO 80523 USA*

[4]*Department of Statistics, Colorado State University, Fort Collins, CO 80523 USA*

[5]*Natural Resource Ecology Laboratory and Department of Ecosystem Science and Sustainability, Colorado State University, Fort Collins, CO, in cooperation with US Geological Survey, Fort Collins Science Center, Fort Collins, CO*

[6]*U.S. Geological Survey (USGS) Earth Resources Observation and Science (EROS) Center, Sioux Falls, SD 57198 USA*

Abstract

Plant population models are powerful tools for predicting climate change impacts in one location, but are difficult to apply at landscape scales. We overcome this limitation by taking advantage of two recent advances: remotely-sensed, species-specific estimates of plant cover and statistical models developed for spatio-temporal dynamics of animal populations. Using computationally efficient model reparameterizations, we fit a spatiotemporal population model to a 28 year time series of sagebrush (*Artemisia* spp.) percent cover over

---
[*]Corresponding author: atredenn@gmail.com

a 2.5 × 5 km landscape in southwestern Wyoming while formally accounting for spatial autocorrelation. We include interannual variation in precipitation and temperature as covariates in the model to investigate how climate affects the cover of sagebrush. We then use the model to forecast the future abundance of sagebrush at the landscape scale under projected climate change, generating spatially explicit estimates of change in a plant population that have, until now, been impossible to produce at this scale. Our broad-scale and long-term predictions are rooted in small-scale and short-term population dynamics and provide an alternative to predictions offered by species distribution models that do not include population dynamics. Our approach, which brings together several common techniques, is among the first steps toward using remote sensing data to model population responses to environmental change that play out at spatial scales far greater than the traditional field study plot.

Key words: population model, climate change, forecasting, spatiotemporal model, remote sensing, sagebrush, Artemisia, *dimension reduction*

Introduction

Forecasting the impacts of climate change on plant populations and communities is a central challenge for ecology (Clark et al. 2001, Petchey et al. 2015). Population models are ideally suited for meeting such a challenge because they provide a way to link climate drivers directly to population dynamics (Hare et al. 2010, Adler et al. 2012, Ross et al. 2015, Shriver 2015). However, inference from population models is typically limited to small spatial extents because the data required is difficult to collect across broad species ranges. Almost every study of plant population dynamics relies on demographic observations recorded at the meter to sub-meter scale (see, e.g., Salguero-Gómez et al. 2015). Local-scale demographic data make building population projection models an easy task (Ellner and Rees 2006, Rees and Ellner 2009, Adler et al. 2012), but it is very difficult

to extrapolate small-scale studies to large spatial extents with any certainty because the data likely only represent a small subset of parameter space and environmental conditions (Freckleton et al. 2011, Queenborough et al. 2011). The real challenge is not to simply make population forecasts, but to do so at spatial scales relevant to policy and management decisions (Queenborough et al. 2011).

The ideal tool would be a large-scale, dynamic population model (Schurr et al. 2012, Merow et al. 2014), but developing useful models at this scale has been limited by the availability of time series data at large spatial extents and statistical methods for fitting high-dimensional spatial models. Fortunately, new advances in remote sensing and statistics now allow us to overcome both of these limitations. First, new remote-sensing (RS) methods are now producing accurate time series of species-specific plant cover at landscape scales. These data can be fit with dynamic population models which include yearly fluctuations in climate as covariates. Such RS time series have revolutionized models of how climate affects ecosystem-level processes (e.g., Running et al. 2004) and have been used to detect long-term trends in plant population abundance (e.g., Homer et al. 2015), but they have yet to be used to drive a dynamic population model. Second, animal population modelers have developed dimension reduction and reparameterization techniques to efficiently fit high-dimension spatiotemporal models (see Conn et al. 2015 for a review). These new statistical methods have yet to be applied to RS-derived plant population data at broad scales.

Large-scale, spatially-explicit population models based on RS data could offer a valuable new way to investigate the effects of large-scale environmental changes playing out at landscape and regional scales. Most current assesments of how plant and animal populations will respond to climate change rely on species distribution models (SDMs). SDMs rely on static associations between contemporary climate and a species' distribution or, more rarely, abundance to project future distribution or abundance (Elith and Leathwick 2009) and they are easily applied at landscape to continental scales (e.g., Maiorano et al. 2013,

76 Clark et al. 2014). However, the short-term and small-scale population dynamics that

77 actually drive the large-scale distributions of species are not represented in most SDMs.

78 Because SDMs typically rely on occurence data, their projections of habitat suitability or

79 probability of occurence provide little information on the future states of populations in

80 the core of their range – areas where a species exists now and is expected to persist in the

81 future (Ehrlén and Morris 2015). Furthermore, because they lack short-term dynamics,

82 SDMs usually cannot produce any estimate of the rate at which local populations will

83 increase or decrease in the near-term and instead project a future equilibrium species dis-

84 tribution that may or may not ever be reached. Direct validation of such predictions is

85 extremely rare (Roberts and Hamann 2012). Large-scale dynamic population models could

86 overcome these limitations. They would produce spatially-explicit estimates of species

87 abundance within the species range (Ehrlén and Morris 2015), have the potential to model

88 expansion in abundance outside the range when coupled with dynamic models of dispersal,

89 and would provide testable predictions of how populations should respond to short-term

90 climate perturbations. These short-term predictions also would give modelers the opportu-

91 nity to repeatedly validate and refine their models (Luo et al. 2011).

92 Sagebrush (*Artemisia* spp.) ecosystems offer an ideal testing ground for new spatially ex-

93 plicit population models derived from RS data. Sagebrush species are widely distributed

94 (Kuchler 1964), they are sensitive to climate (Perfors et al. 2003, Miglia et al. 2005, Poore

95 et al. 2009, Dalgleish et al. 2011, Xian et al. 2012, Apodaca 2013, Schlaepfer et al. 2014a,

96 2014b, Harte et al. 2015, Homer et al. 2015), new landscape and regional scale time series

97 of sagebrush cover are now being produced from aerial imagery (Homer et al. 2012), and

98 forecasts of future sagebrush ecosystems are in high demand due to the precarious conser-

99 vation status of the greater sage-grouse (*Centrocercus urophasianus*) (Arnett and Riley

100 2015). SDMs typically predict that much of the area occupied by sagebrush ecosystems

101 today will become unsuitable for sagebrush due to climate change, resulting in a dramatic

102 loss in the extent of sagebrush habitat by the end of this century (Shafer et al. 2001, Neil-

4

son et al. 2005, Bradley 2010, Schlaepfler et al. 2012, Still and Richardson 2015). Eco-hydrology models supply a possible mechanism for sagebrush losses predicted by SDMs: climate warming could lead to earlier snowmelt, increased evaporation and ultimately less recharge of deeper soil layers in the spring (Schlaepfler et al. 2012, Schlaepfer et al. 2014a). In warmer parts of its range, increased temperature could be especially detrimental to sagebrush as it depends on water from deeper soil to survive and grow in this arid region (Pechanec et al. 1937, Schlaepfer et al. 2011, Germino and Reinhardt 2014). In contrast, at higher elevations and in colder regions, warming and earlier snowmelt could lengthen the growing season and increase sagebrush occurrence (Schlaepfler et al. 2012, Schlaepfer et al. 2014a). Direct observations of individual plants and experimental plots tend to agree with these models: growth tends to respond negatively to spring and summer temperatures (Miglia et al. 2005, Poore et al. 2009, Apodaca 2013) except at higher elevations where earlier snowmelt may allow for a longer growing season (Perfors et al. 2003, Harte et al. 2015). A large-scale, spatially-explicit population model for sagebrush driven by interannual climate variability would provide a valuable new tool for assessing how sagebrush could respond to climate change in the future.

Building on recent technological advances in spatial statistics (Latimer et al. 2009, Conn et al. 2015) and anticipating ever-increasing availability of RS data (He et al. 2015), we demonstrate how large-scale plant population models could be used to predict population impacts of climate change. As a proof-of-concept, we use a process model motivated by Gompertz density-dependent population growth and a remotely-sensed time series of sagebrush cover from Wyoming (Homer et al. 2012, 2015). We account for spatial autocorrelation with dimension reduction techniques (Latimer et al. 2009, Conn et al. 2015) and produce spatially-explicit estimates of sagebrush percent cover. Unlike most SDMs, our approach models the dynamics of plant abundance through time, and thus, is a population model, in the same spirit that models of animal counts through time are population models. The modeling framework we propose can be applied to any spatially-explicit time

series of plant cover or density, but its application to remotely-sensed data products offers
the greatest potential to combine the information of population models (e.g., population
status and temporal dynamics) and the spatial extent of species distribution models.

Materials and Methods

Data

Remotely-sensed time series   To demonstrate our modeling approach, we use a
subset of a remotely-sensed time series of sagebrush (*Artemisia* spp.) canopy cover in
Wyoming (Homer et al. 2012). As part of a separate study, Homer et al. 2012 estimated
sagebrush percent cover using a regression tree to relate ground reflectances retrieved
by three sources of optical imagery (QuickBird, Landsat, and AWiFS) to 1,780 field
observations of sagebrush cover distributed across Wyoming. The regression tree model
was further validated using another 297 field observations. For Wyoming sagebrush, the
model achieved an $R^2 = 0.65$ and an out-of-sample RMSE of 5.46% (Homer et al. 2012).
To hind-cast sagebrush cover the regression tree model was applied to historical remote
sensing images to generate yearly predictions of sagebrush cover for all of Wyoming for
the years 1984-2011. This resulted in an annual time series of sagebrush cover at 30
meter resolution from 1984 to 2011 (Fig. B1). In this remote sensing product, values
represent the percentage of a 30×30 meter pixel covered by sagebrush. In our study, we
focused on a $5,070 \times 2,430$ meter subset totaling $13,689$ 30×30 meter pixels each year
(Fig. 1). Thus, the full remote sensing product contains 369,603 observations spanning 27
year-to-year transitions (27 years $\times$ 13,689 pixels).

Climate covariates   Our approach models interannual changes in plant cover as a func-
tion of seasonal climate variables. We used daily historic weather data for the center of

6

our study site from the NASA Daymet data set (*available online*)[1]. The Daymet weather data are interpolated between coarse observation units and capture some spatial variation. We relied on weather data for the centroid of our study area. We calculated five climate variables from the Daymet data for the time period coinciding with our remotely sensed data (1984 to 2011).

We narrowed our focus to climate covariates we know are important for sagebrush and that could be calculated from general circulation model projections. The five climate variables in our population model are: (1) cumulative, "water year" precipitation for year *t*-2 (*lagPpt*), (2) year *t*-1 fall through summer precipitation (*ppt1*), (3) year *t* fall through summer precipitation (*ppt2*), (4) year *t*-1 average spring temperature (*TmeanSpr1*), and (5) year *t* average spring temperature (*TmeanSpr2*), where *t-1* to *t* is the transition of interest. We selected these variables *a priori* based on previous studies (see *Introduction*), though not all emerge as important predictors in our model.

Additive spatio-temporal model for sagebrush cover

We use a descriptive model for sagebrush cover that includes additive spatial and temporal effects similar to that described by Conn et al. (2015). Interannual change in percent cover represents the integrated outcome of recruitment, survival, growth, and retrogression (shrinkage) of individual plants from year to year. We model observed integer percent cover (y) in cell i at time t as conditionally Poisson

$$y_{i,t} \sim \text{Poisson}(\mu_{i,t}), \tag{1}$$

where $\mu_{i,t}$ is the expected percent cover of pixel i in year t

$$\log(\mu_{i,t}) = \underbrace{\beta_{0,t} + \beta_1 y_{i,t-1}}_{\text{temporal + dens. dep}} + \underbrace{\mathbf{x}'_t \boldsymbol{\gamma}}_{\text{climate}} + \underbrace{\eta_i}_{\text{spatial}}. \tag{2}$$

Our model of percent cover change includes a density-dependent effect of log-transformed cover in the previous year ($y_{i,t-1}$), climate effects ($\mathbf{x}_t$), and a spatial random effect (η) for

---

[1]http://daymet.ornl.gov/

7

177 each pixel i. Climate effects were standardized $[(x_i - \bar{x})/\sigma(x)]$ to improve convergence during

178 the model fitting stage and to allow for easier prior specification. The intercept, $\beta_{0,t}$, was

179 allowed to vary through time; these random year effects recognize that all observations

180 from a particular year share the same climate covariates and thus are not independent.

181 We used a Poisson likelihood because integer percent cover values in the sagebrush data

182 product can be considered a form of count data. We also evaluated a negative binomial

183 model, but found little evidence for overdispersion beyond what our model was already

184 accomodating via the spatial random effects ($\boldsymbol{\eta}$). There was no evidence of zero-inflation

185 in our data, but see below (*Accomodating zeros*) for how we handled the small number

186 of zero percent cover observations. We assume that the remotely sensed estimates of per-

187 cent cover are "true" and free of error. This need not be the case, and if measurement or

188 sampling error is known then it could be included in our Bayesian model as a "sampling

189 model" (Hobbs and Hooten 2015).

190 The spatial random effect ($\boldsymbol{\eta}$) accounts for spatial autocorrelation among pixels that occur

191 near each other in space. Thus, $\boldsymbol{\eta}$ acts as an offset on the intercept ($\beta_{0,t}$), creating a spa-

192 tial field that defines how pixels differ from the mean, on average, in space (e.g., areas of

193 perennially low or high cover, relative to average cover). Fitting the model with a spatial

194 random effect (η) is computationally demanding for large data sets like ours. The com-

195 putational demand is due to the required calculations of the spatial covariance matrices,

196 which increase as a cubic function of the number of locations (Wikle 2010). Key to our

197 approach is a dimension reduction strategy that greatly reduces the number of parameters

198 needed to be estimated to account for spatial variation by reducing the size of the spatial

199 covariance matrices that need to be inverted at each MCMC iteration. Fitting models that

200 appropriately account for spatial autocorrelation over large spatial extents would not be

201 feasible without these modern techniques. Our dimension reduction strategy expresses the

202 high dimensional spatial random effect, $\boldsymbol{\eta}$, as the product of an expansion matrix, $\mathbf{K}$, and

203 a smaller parameter vector, $\boldsymbol{\alpha}$ (e.g., Hooten et al. 2003, Hooten and Wikle 2007, Conn et

al. 2015). We can then approximate the spatial effect as

$$\boldsymbol{\eta} \approx \mathbf{K}\boldsymbol{\alpha}, \tag{3}$$

$$\alpha_m \sim \text{Normal}(0, \sigma_\eta^2). \tag{4}$$

In this case, $\boldsymbol{\alpha}$ is a $m \times 1$ vector of reduced spatial random effects, and $\mathbf{K}$ is a $S \times m$ matrix that maps the reduced effects to the full S-dimensional space, where S is the total number of observed locations. Thus, we are able to reduce the effective number of parameters from S to m.

The last remaining obstacle is to parameterize the matrix of basis functions, $\mathbf{K}$. We use kernel convolution (Barry and Hoef 1996, Higdon 1998) to interpolate the spatial random effect between m "knots" that are nonrandomly distributed across the space of our study area. This means we are modeling spatial random effects at the knot level, and we use $\mathbf{K}$ to interpolate those effects between knots. We use an exponential kernel density to define the distance-decay function around the knots ($\mathbf{w}$), such that the entries of $\mathbf{K}$ are

$$K_{s,m} = w_{s,m} / \sum_{s=1}^{S} w_{s,m} \tag{5}$$

where

$$w_{s,m} = \exp\left(\frac{-d_{s,m}}{\sigma}\right) \tag{6}$$

and $d_{s,m}$ is the Euclidean distance between the centroid of sample cell s and the location of knot m, and σ is the kernel bandwidth. It is possible, through exhaustive model selection and fitting, to determine the optimal form of the kernel and to estimate optimal values for σ (Higdon 2002, Hooten and Hobbs 2015). However, given the relative size of our dataset and computational limitations, we defined kernels around 231 knots (Fig. C2) whose nearest neighbor distances are approximately equal to the range of spatial dependence in residuals from a simple GLM fit without climate covariates and the spatial random effect (~500 meters; Appendix C). An infinite number of knots would result in an exact representation of the spatial process and covariance model. Computationally, using an infinite number of knots is not possible, thus the use of dimension reduction techniques

9

229 serves as an approximation, where the accuracy increases with the number of knots. Given

230 the tradeoff between knot number and computation time, we chose to base our knot num-

231 ber on the spatial dependence as described above.

232 The Bayesian posterior distribution of our spatio-temporal model can be expressed as

$$[\boldsymbol{\beta}, \boldsymbol{\gamma}, \boldsymbol{\alpha}, \sigma_\eta^2 | \mathbf{y}] \propto \left(\prod_{t=1}^T \prod_{i=1}^n [y_{i,t} | \beta_{0,t}, \beta_1, \boldsymbol{\gamma}, \boldsymbol{\alpha}][\beta_{0,t} | \bar{\beta}_0, \sigma_{\beta_0}^2] \right) \times \tag{7}$$

$$\left(\prod_{m=1}^M [\alpha_m | \sigma_\eta^2] \right) [\bar{\beta}_0][\beta_1][\boldsymbol{\gamma}][\sigma_{\beta_0}^2][\sigma_\eta^2].$$

233 Accomodating zeros

235 Our process model (in Eq. 2) includes a log transformation of the observations ($\log(y_{t-1})$).

236 Thus, our model does not accomodate zeros. Fortunately, we had very few instances where

237 pixels had 0% cover at time *t-1* ($N = 47$, which is 0.01% of the data set). Thus, we ex-

238 cluded those pixels from the model fitting process. However, when simulating the process,

239 we needed to include possible transitions from zero to non-zero percent cover. We fit an

240 intercept-only logistic model to estimate the probability of a pixel going from zero to non-

241 zero cover

$$y_i \sim \text{Bernoulli}(\mu_i) \tag{8}$$

$$\text{logit}(\mu_i) = b_0 \tag{9}$$

243 where **y** is a vector of 0s and 1s corresponding to whether a pixel was colonized ($>0\%$

242
244 cover) or not (remains at 0% cover) and μ_i is the expected probability of colonization as

245 a function of the mean probability of colonization (b_0). We fit this simple model using the

246 'glm' command in R (R Core Team 2013). For data sets in which zeros are more common

247 and the colonization process more important, the same spatial statistical approach we used

248 for our cover change model could be applied and covariates such as cover of neighboring

249 cells could be included.

Fitting the model

We fit the spatiotemporal model in R (R Core Team 2013) using the 'No-U-Turn' Hamiltonian Monte Carlo sampler in Stan (Stan Development Team 2014a) and the RStan package (Stan Development Team 2014b). We obtained posterior distributions of all model parmaters from three MCMC chains comprised of 1,000 iterations each, after discarding an initial 1,000 iterations as burn in. Short chains of samples are a hallmark of the Stan algorithm, which is extremely efficient. Compared to other samplers, fewer iterations are required to achieve convergence. Each chain was initialized with unique parameter values and the model was fit in parallel using the Utah State University High-Performance Computing facility. Model fitting required five days on a four node Central Processing Unit with $2 \times$ AMD Opteron(tm) Processor 4386 @ 3.10 Ghz, 64GB of RAM per node, 16 cores per node, and each chain launched in parallel on separate cores. We assessed convergence visually and calculated scale-reduction factors (Appendix D, $\hat{R} < 1.1$ for all parameters) (Gelman and Rubin 1992, Gelman and Hill 2009).

Simulating the process

We performed four sets of simulations to (1) compare observed and simulated equilibrium cover, (2) compare observed and simulated year- and location-specific cover, (3) forecast future equilibrium population states under projected climate change, and (4) make temporally-explicit forecasts of sagebrush cover starting the final year of our observations and ending in year 2098. Using the posterior distribution of model parameters, we simulated a matrix of pixels equal to the size of the study area (13,689 pixels or matrix elements). For simulations (1) and (3) we initialized all pixels with arbitrarily low cover (1%) and then projected the model forward by randomly drawing climate covariates from the observed climate time series (for 1) or a perturbed climate time series (for 3). We ran equilibrium simulations (1 and 3) for 2,000 time steps and then compared the output across

11

₂₇₅ simulations, after discarding an initial 100 time steps. To calculate average future equilib-

₂₇₆ rium sagebrush cover, we ran simulation (3) for each GCM and RCP scenario separately,

₂₇₇ and then averaged the results over GCMs. For simulation (2), we initialized each pixel

₂₇₈ with its actual percent cover value for time t and cell s and projected the model forward

₂₇₉ one time step and compared the one-step ahead forecast with the observed value. For

₂₈₀ simulation (4), we initialized each pixel with the final observed value in 2011 and then

₂₈₁ projected the model forward based on GCM yearly weather projections. We ran these sim-

₂₈₂ ulations for each GCM and RCP scenario combination separately and then aggregated

₂₈₃ the results over the GMCs by calculating the mean and the 90th percentiles for each RCP

₂₈₄ scenario.

₂₈₅ We used the posterior mean of each parameter for all simulations except for (4) where we

₂₈₆ ran 50 simulations with unique sets of parameters from the chains. Random year effects

₂₈₇ were included in simulations by randomly drawing a posterior mean year effect ($\beta_{0,t}$) for

₂₈₈ each iteration (simulations 1 and 3), using the posterior mean year effect for a specific year

₂₈₉ (simulation 2), or by a drawing a future-year random effect from the posterior mean and

₂₉₀ standard deviation of the mean intercept (simulation 4, e.g., $\beta_{0,T} \sim \text{normal}(\bar{\beta}_0, \sigma^2_{\beta_0})$ for

₂₉₁ some future year T). Our simulation approach provides a reasonable and computationally

₂₉₂ efficient approximation to the true posterior predictive mean when used in these scenarios

₂₉₃ with our data.

₂₉₄ We required future projections of climate for our study area to conduct the equilibrium

₂₉₅ and temporally-explicit forecasts described above. Thus, we used the most recent climate

₂₉₆ projections from the Intergovernmental Panel on Climate Change (IPCC), the Coupled

₂₉₇ Model Intercomparison Project 5 (CMIP5; *available online*)[2]. The CMIP5 provides pro-

₂₉₈ jections from a suite of global circulations models (GCMs); we used projections from 18

₂₉₉ GCMs (Table A1) that produced weather projections for three "Representative Concen-

---

[2]http://cmip-pcmdi.llnl.gov/cmip5/

tration Pathways": RCP 4.5, RCP 6.0, and RCP 8.5 (*described online*)[3]. The three RCPs correspond to stabilization of radiative forcing before 2100, after 2100, and ongoing increase in greenhouse gas emissions, respectively.

To simulate equilibrium sagebrush cover under projected future climate we applied average projected changes in precipitation and temperature to the observed climate time series. For each GCM and RCP scenario combination, we calculated average precipitation and temperature over the 1950-2000 time period and the 2050-2098 time period. We then calculated the absolute change in temperature between the two time periods (ΔT) and the proportional change in precipitation between the two time periods (ΔP) for each GCM and RCP scenario combination. Lastly, we applied ΔT and ΔP to the observed 28-year climate time series to generate a future climate time series for each GCM and RCP scenario combination. These generated climate time series were used to simulate equilibrium sagebrush cover. We simulated equilibrium cover separately for each GCM and RCP scenario combination before averaging the results, but we show the average projected climate changes across all models in Table 1.

For the temporally-explicit forecasts we used yearly GCM projections from 2012 to 2098 to simulate the process starting from the end point of the remotely sensed sagebrush cover data (ends in 2011). We aggregated daily GCM output for each GCM and RCP scenario into the seasonal climate covariates used to fit our model. These yearly climate time series were not aggregated further because we ran simulations for each GCM and RCP scenario, rather than one simulation per RCP scenario averaged over GCMs. Note that forecasting with our model, which relies on historical correlations between sagebrush cover change and weather, using future climate projections requires assuming such relationships remain in the future.

---

[3]http://tntcat.iiasa.ac.at/RcpDb/

Results

Averaging across all GCMs, precipitation and temperature in our study area are projected to increase; the magnitude of increase depends on the RCP scenario (Table 1). Trajectories of our climate covariates from GCM projections show similar trends (Fig. 2).

All parameters in our model converged on stable posterior distributions (Appendix D). Only the *lagPpt* climate covariate can be considered important based on a 90% credible interval, and it had a positive effect on sagebrush percent cover change (Fig. 3). In other words, if the year 2000 water year was wetter than average, sagebrush cover would increase from the 2001 to the 2002 growing season. Other climate effects strongly overlapped zero but their posterior means were positive, except for fall-through-spring precipitation the first year of a cover transition (t-1), whose posterior mean was negative (Fig. 3). The posterior mean for the spatial random effect, $\boldsymbol{\eta}$, captured the overall spatial structure of the observed data (Fig. E1). This indicates our choice of knot placement and dimension reduction strategy was adequate for describing permanent spatial variation in the data.

When we simulated the pixel-based population model based on observed climate, it was able to reproduce the spatial pattern of observed percent cover, averaged over time (Fig. 4A,B). Our model shows a tendency to underpredict perennially-low percent cover pixels (Fig. 4C), but does a better job at predicting high cover pixels. Point predictions are most confident, though slightly biased, in low percent cover pixels (Fig. 4D). The model is also able to adequately reproduce observed dynamics when we make one-step-ahead predictions based on observed climate and cover in the previous year for each pixel. When we made these in-sample, one-step-ahead forecasts, the model achieved an RMSE = 4.31, in units of percent cover. The Pearson's correlation between observations and predictions was 0.62.

When we apply the fitted model to IPCC climate change scenarios, the model predicts gains in sagebrush percent cover, on average (Figs. 5, 6A). The spatial effect remains strong enough in low cover regions to counteract the positive effect of projected precip-

14

itation increases (Fig. 5). Thus, our model predicts an increase in the heterogeneity of sagebrush cover because projected cover increases are smaller in low cover pixels than in high cover pixels (Fig. 5 and Fig. F1). For the temporally-explicit forecasts, we show spatially-averaged values and the associated uncertainty due to variability in GCM projections, variability in model parameters, and uncertainty in our process model (Fig. 6A). Based on our model and GCM projections, we forecast an average increase in sagebrush cover at our study area, but a decrease is not outside the realm of possibility (shaded regions in Fig. 6A). The generally increasing trend reflects the positive effect of precipitation on sagebrush cover change estimated for our study area (Fig. 3). We also show how our model is capable of near-term forecasts in Fig 6B.

Discussion

Despite the need to forecast population responses to climate change over large spatial extents, as demonstrated by the wide application of species distribution models (e.g., Clark et al. 2014), landscape-scale population models for plant species remain more concept than reality (Schurr et al. 2012, Merow et al. 2014). We introduced a new approach that uses methods from the dynamic spatio-temporal modeling literature (e.g., Conn et al. 2015) to fit a population model to remotely-sensed estimated of plant percent cover. As a proof-of-concept, we applied our approach to a remotely-sensed data product of sagebrush percent cover from 1984 to 2011 in Wyoming (Homer et al. 2012). We first discuss our results specific to sagebrush ecology and response to climate, and then discuss the more general implications and limitations of our proposed approach.

Sagebrush response to climate and climate change

The climate effects we estimated, based on cover data at 30 meter spatial resolution, are consistent with individual-level responses of sagebrush to climate-related variables. Re-

15

374 search on individual plants has shown that wetter winters are correlated with greater stem

375 growth in sagebrush (Poore et al. 2009, Apodaca 2013) and that warmer spring tempera-

376 tures may enhance sagebrush growth in cold climates by advancing the date of snowmelt

377 and increasing the length of the growing season (Perfors et al. 2003, Harte et al. 2015).

378 In agreement with those individual-level responses, posterior means for all precipitation

379 and temperature effects in our model were positive, except for the effect of fall-through-

380 spring precipitation in the first year of a cover transition (*ppt1*, Fig. 3). The cumulative

381 amount of precipitation the year before a cover transition (*pptLag* in our model) emerged

382 as the strongest predictor of sagebrush cover change (Fig. 3). However, mean estimates

383 for the climate effects are relatively weak (Fig. 3). Such small effects could indicate that

384 sagebrush are not very sensitive to interannual climate variability, that our model is poorly

385 specified, or that climate responses are difficult to detect using coarse-scale data. Given

386 findings from previous research demonstrating the importance of precipitation and tem-

387 perature to sagebrush growth (Pechanec et al. 1937, Schlaepfer et al. 2011, Germino and

388 Reinhardt 2014) and regeneration (Schlaepfer et al. 2014b), it is unlikely that sagebrush

389 are insensitive to climate. We used aggregated climate covariates that may not completely

390 capture the climate-dependence of sagebrush cover change. However, the covariates we

391 chose closely match the climate-related variables that have been shown to drive sagebrush

392 growth, survival, and regeneration (e.g., Dalgleish et al. 2011, Schlaepfer et al. 2014b).

393 More likely, aggregated estimates of plant abundance, such as percent cover, mask inter-

394 annual variability at the level of the individual plant and makes it more difficult to detect

395 the drivers of internanual variability. Additionally, we chose not to downscale the Daymet

396 weather data, meaning that in a given year all pixels shared the same climate, which limits

397 our statistical power. Nonetheless, our model was capable of detecting climate effects

398 that agree with our knowledge of sagebrush ecology and allowed us to make forecasts of

399 future sagebrush abundance.

400 Under projected climate, we forecast modest increases in sagebrush cover for all RCP

16

scenarios in the long-term (Figs. 5,6A). Our forecasts reflect both the estimated effect size for each climate covariate and the amount of change in those covariates projected by the GCMs. Cumulative precipitation the year before a given year-to-year transition was the strongest standardized effect (Fig. 3), but precipitation is projected to increase only moderately (Table 1, Fig. 2) and the negative effect of fall-through-spring precipitation in the first year of a cover transition (*ppt1*) had an offsetting effect. In contrast, mean spring temperature had a weak positive effect on sagebrush cover changes, but the projected temperature increase is large (Table 1, Fig. 2).

An interesting consequence of explicitly modeling the effect of space (through $\boldsymbol{\eta}$) is the forecasted increase in spatial heterogeity (Fig. F1). Our model projects little change in low cover pixels but substantial increases in the cover of high cover pixels (Fig. 5). Had we not explicitly accounted for spatial-dependence in our model, we would have missed this result. We were unable to attribute the spatial structure apparent in the data (Fig. 4A) and approximated by our model ($\boldsymbol{\eta}$, Fig. E1) to slope, aspect, elevation, or coarse soil type (results not shown). The lack of correlation between $\boldsymbol{\eta}$ and landscape factors leads us to conclude that the spatial structure in our data set emerges from some combination of fine-scale microhabitat associations and legacy effects related to fire and species invasions.

While we forecast an increase in sagebrush cover at our study area, SDM studies typically project dramatic declines in climate suitability for sagebrush with warming (Shafer et al. 2001, Neilson et al. 2005, Bradley 2010, Schlaepfler et al. 2012, Still and Richardson 2015). There are many potential explanations for this apparent contrast, ranging from the type of model used to the particular climate covariates considered, but the location of our study area in a cold portion of sagebrush's geographic distribution may be the best. The response of plant species to weather varies along climatic gradients (e.g., Clark et al. 2011, Vanderwel et al. 2013), and sagebrush are especially sensitive to the timing of snowmelt because their growth depends on recharge of deep soil water (Schlaepfler et al. 2012, Schlaepfer et al. 2014a). In warmer parts of the sagebrush range, earlier snowmelt is

17

detrimental to growth and survival (Pechanec et al. 1937, Schlaepfer et al. 2011, Germino and Reinhardt 2014). In colder regions, earlier snowmelt due to temperature increases can lengthen the growing season and increase sagebrush occurence and cover (Schlaepfler et al. 2012, Schlaepfer et al. 2014a). The average annual temperature across the sagebrush steppe biome is 6.9°C (sd = 1.6; Schlaepfer et al. 2011), whereas average temperature at our study area from 1980 to 2013 was 4.6°C (calculated from Daymet estimates). Our study area lies at the cold extreme of the sagebrush range, thus the weak positive response to temperature that we estimated (Fig. 3) and carried through to our forecasts (Figs. 5,6A) likely represents the positive effect of earlier snowmelt, and thus higher moisture availability early in the growing season.

A previous analysis of a different subset of the remote sensing data set we used also came to a different conclusion, projecting future sagebrush decline (Homer et al. 2015). The discrepancy between the results of Homer et al. (2015) and ours primarily reflects a difference in the climate projections used for projecting future changes rather than differences in our inference about responses to historical variation in weather. Homer et al. (2015) used downscaled weather projections from a single model from the IPCC 4 whereas we used native-resolution weather projections from a suite of models from the IPCC 5. Consistent with our study, Homer et al. (2015) found a generally positive relationship between pixel-level sagebrush cover and precipitation, but the future climate scenario they chose resulted in a mean decrease in precipitation, causing a predicted decline in sagebrush cover. A second difference is that Homer et al. (2015) relied on regressions of decadal trends in sagebrush cover against decadal trends in climate at the level of individual pixels. Our current approach is fundamentally different in that we specifically model the impact of interannual variation in weather on year-to-year changes in sagebrush cover using a dynamic population model. Thus, our model takes advantage of the additional information contained within short-term responses to climate fluctuations. Lastly, the location of Homer et al.'s (2015) study area is, on average, at a lower elevation than our current study area.

The geographic difference results in different historical and projected climate, and, as discussed above, sagebrush may respond differently to warming depending on geographic location.

We projected sagebrush cover to the end of this century, but an important feature of our approach is that it can also produce short-term forecasts (Fig. 6B). For example, we could forecast the effects of a multi-year regional drought on sagebrush cover (Debinski et al. 2010). Validating spatial population models against short-term predictions would give ecological forecasters a way to assess and improve the performance of their models, which would greatly increase our confidence in long-term forecasts. This cycle of prediction, validation, and refinement is missing from most currently available population-level forecasts of the effects of climate change.

A landscape-scale plant population modeling approach: opportunities and limitations

Our approach for modeling plant populations overcomes two major hurdles for spatially-explicit population models. First, we used moderate resolution, remotely-sensed estimates of sagebrush percent cover as a response variable, enabling us to fit a dynamic population model over a large spatial extent. Species-specific estimates of plant abundance are becoming commonplace as remote sensing technology develops (e.g., Baldeck and Asner 2014, Colgan and Asner 2014), and in a few years several remotely-sensed time series may be available. Second, borrowing from new methods in spatio-temporal modeling of animal abundance (e.g., Conn et al. 2015), we fit the model using a dimension reduction strategy that accounted for spatial autocorrelation within a feasible computational time. Accounting for spatial autocorrelation allows for statistically rigorous inference on the effects of interannual climate on sagebrush cover change in our study region. The spatial covariance structure also provided a way to obtain spatially-explicit predictions at a resolution be-

low that of the climate covariates (i.e., within the study region; Figs. 4,5). Our approach is amenable to any spatially-explicit time series of plant abundance, but we see remote-sensing datasets offering the largest opportunity for landscape-scale population models. Furthermore, it would be straighforward to include additional covariates related to disturbance (e.g., fire) or biotic interactions. Thus, we see our method as a first step toward coupling the mechanistic power of dynamic population models with the spatial extent of SDMs. The spatially- and temporally-explicit forecasts made possible by our approach should be especially relevant to land management decisions based on near-term forecasts.

Several *a priori* modeling decisions determined the spatial extent and resolution of our results. We retained the native spatial resolution of the remote sensing data (30×30 meters). This constrained the extent that we could reasonably model because of the computational challenges in estimating spatial random effects. Even with our dimension reduction technique, modeling a larger area at this resolution would require a greater number of spatial knots, and computation time would increase substantially (Wikle 2010). To model a larger spatial extent, we could aggregate the original remote-sensing time series data to a coarser spatial resoluation. This would allow us to model a much greater spatial extent with a similar number of knots and a similar computation time. While a coarser scale model would lose some fine-scale detail, it could be applied to a much larger area, potentially gaining some strength in estimating climate effects by spanning a greater range of climate variation. However, gains made by incorporating greater regional variability by modeling at a coarser resolution could be offset by the loss of information inherent when aggregating plant responses into larger pixels.

Our spatial extent and resolution also affected our use of climate covariates. We did not downscale Daymet data to match the spatial resolution of the sagebrush data, meaning that in each year all pixels share the same climate covariates. This is a potential limitation of our study, and could explain the weak effect of climate covariates that we observed (Fig. 3). We also did not allow different portions of our study area to respond to climate

20

in different ways. Doing so would require spatially-varying climate effects and a substantial increase in computational time. However, in future applications, it will be important to allow climate effects to vary over space to better capture reality. Conn et al. (2015) provide examples of how such spatiotemporal interactions can be included in abundance models. We might expect climate effects to interact with spatial covariates such as soil type, slope, and aspect. In our relative small study area, we did not observe important effects of these factors, but it is possible to include such abiotic data layers as predictors when fitting models at larger spatial extents where variability may be greater.

The uncertainty associated with our forecasts highlights several opportunities to improve our approach. First, parameter uncertainty could be reduced by regulating the variance of the posterior distributions of climate covariates via ridge regression (e.g., Gerber et al. 2015). Second, uncertainty associated with climate projections could be reduced by identifying GCMs that perform exceptionally well for a particular study location (e.g., Rupp et al. 2013). Such considerations will be important when forecasting in support of particular management objectives. However, knowledge of uncertainty is itself important knowledge for management (Bradshaw and Borchers 2000). Deciding that no management actions should be taken based on the data at hand is itself a management decision.

Conclusion

We introduced a new approach to fitting and simulating population models at large spatial extents with plant population data derived from state of the art remote sensing. We used the model to forecast future abundances of sagebrush in Wyoming and found that at our relatively cold site sagebrush should be expected to increase in cover. As more species-level remote sensing datasets become available and computing power increases this approach will be applicable to a wider number of species and even larger spatial extents. Future modeling could include the effects of non-climate drivers – including the effects of

21

species interactions and disturbance. For sagebrush, including fire and competition with non-native annual grasses in the model may be especially important for a complete assesment of the effects of climate change (Bradford and Lauenroth 2006). Fortunately, our spatio-temporal modeling framework could easily be extended to model additional species and dynamic processes as the data become availabe. The approach we have developed here fills an important gap in spatial scales between species distribution models and local-scale demographic population models.

Acknowledgments

557 Organization for Earth System Science Portals. Any use of trade, firm, or product names

558 is for descriptive purposes only and does not imply endorsement by the U.S. government.

Tables

Table 1: Projected changes in temperature and precipitation at our study area from CMIP5 average GCM projections for 2050-2100 relative to average temperature and precipitation from 1950-2000.

Emissions Scenario	Absolute change in temperature	Percentage change in precipitation
RCP 4.5	2.98°	8.94%
RCP 6.0	3.13°	8.64%
RCP 8.5	4.79°	11.0%
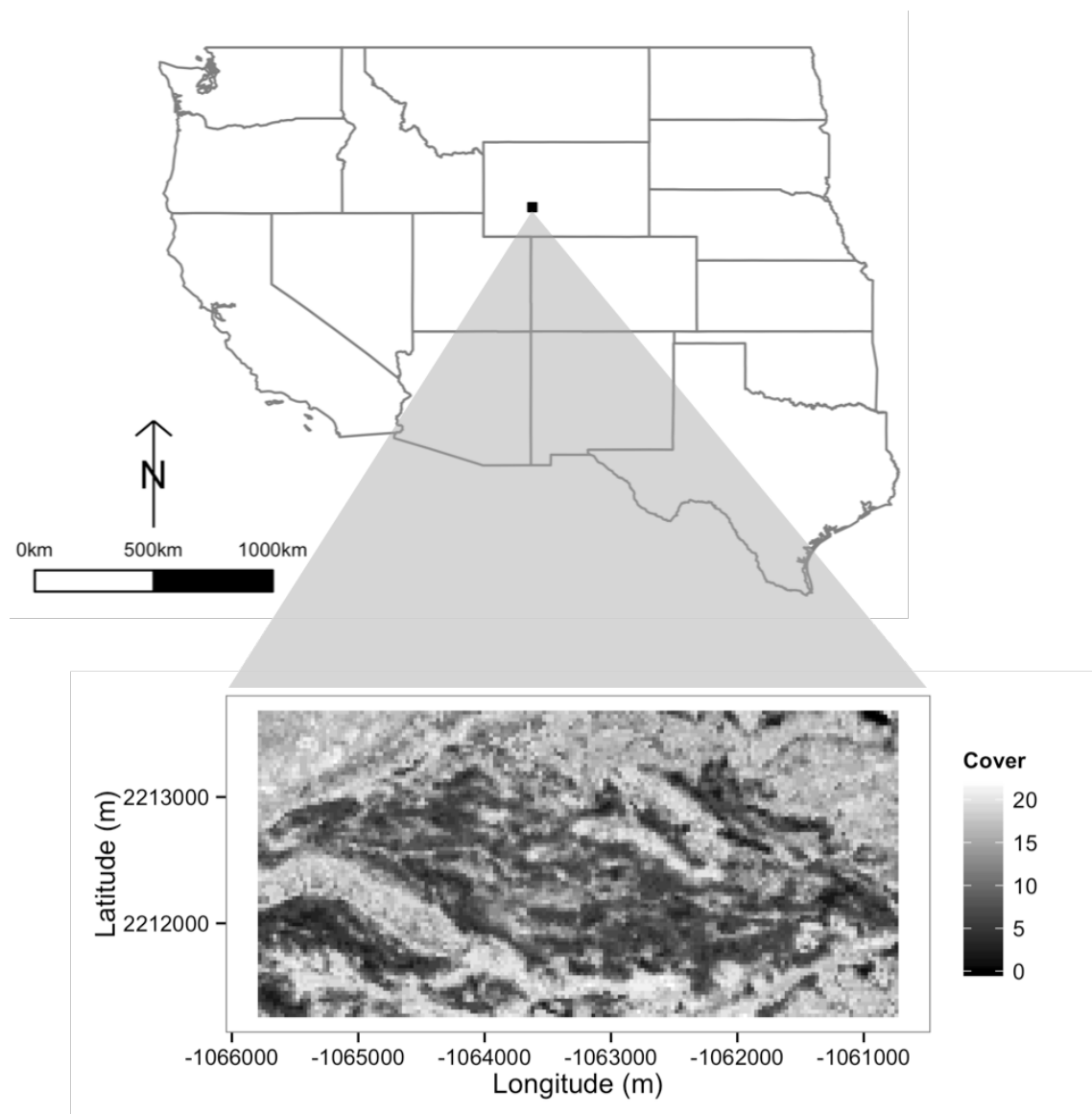
Figures

Figure 1: Location of the 5,070 × 2,430 meter kilometer study area in southwestern Wyoming (black rectangle) and a snapshot of the percent cover data in 1984 (detailed inset). Scale bar is relevant for US map only; refer to axes labels on the detailed inset of sagebrush percent cover for scale of the study area.
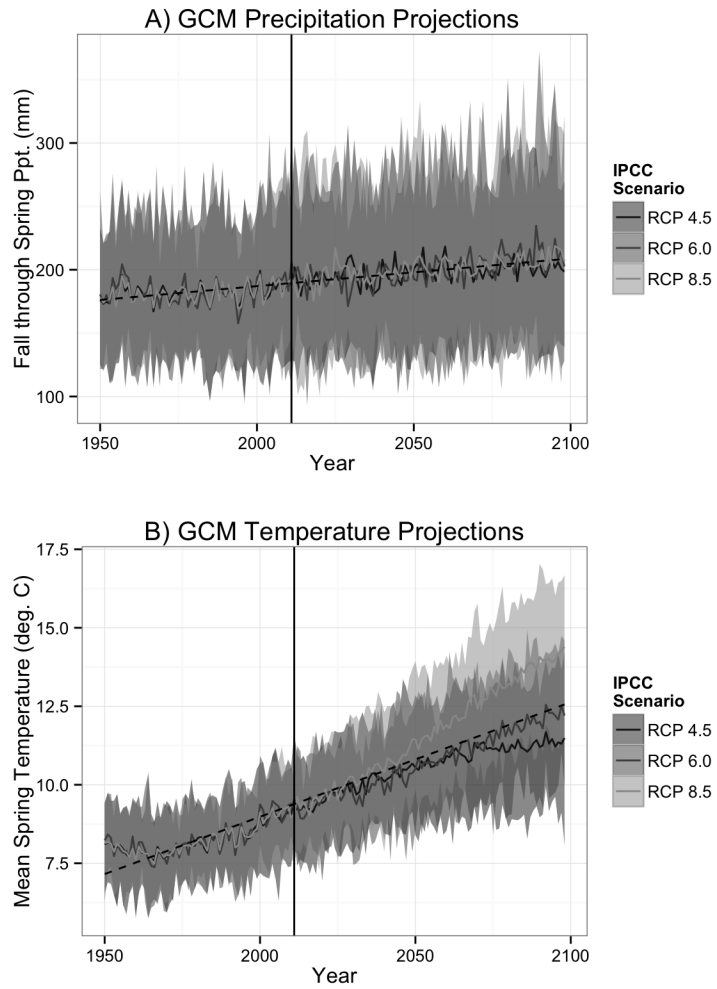
Figure 2: GCM yearly weather hindcasts (before solid line at 2011) and projections (after solid line at 2011) for precipitation (A) and temperature (B) at our study area in south-western Wyoming (see Fig. 1).
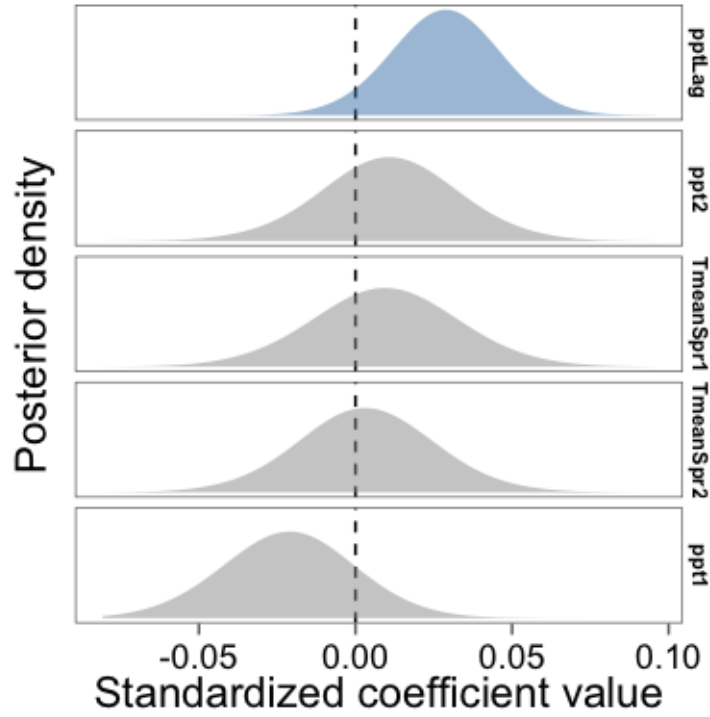
Figure 3: Posterior distributions of climate covariates. The x-axis is the standardized coefficient value because we fit the statistical model for sagebrush cover change (Eq. 7) using standardized covariate values. Only cumulative precipitation at time *t-2* (pptLag) is important (shown in blue; 90% CI does not overlap zero). Climate covariate codes: pptLag = water year precipitation in year *t-2*; TmeanSpr1 = year *t-1* average spring temperature; ppt2 = year *t* fall through summer precipitation; TmeanSpr2 = year *t* average spring temperature; ppt1 = year *t-1* fall through summer precipitation.
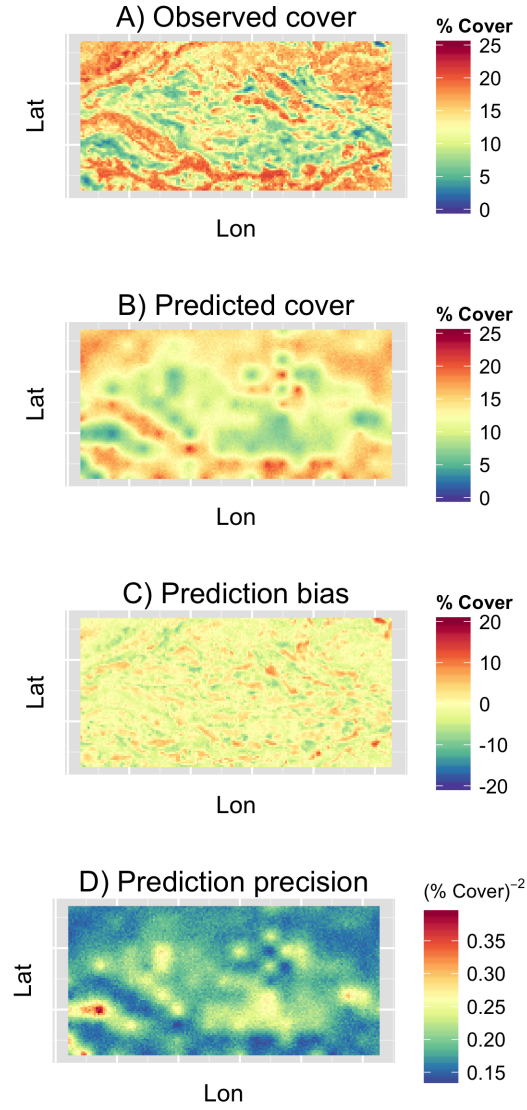
Figure 4: Observed and predicted (A, B) equilibrium percent cover of sagebrush, and prediction bias and precision (C, D) for the extent of our spatial area at 30-m resolution. Observed equilibrium sagebrush cover (A) is the temporal mean of each pixel from the 28 year time series. Prediction results are from simulations that use posteior mean parameter values. Precision in (D) represents the variability of each pixel over the course of the 2,000 iteration simulation. Axes definitions: Lat = latitude; Lon = longitude.
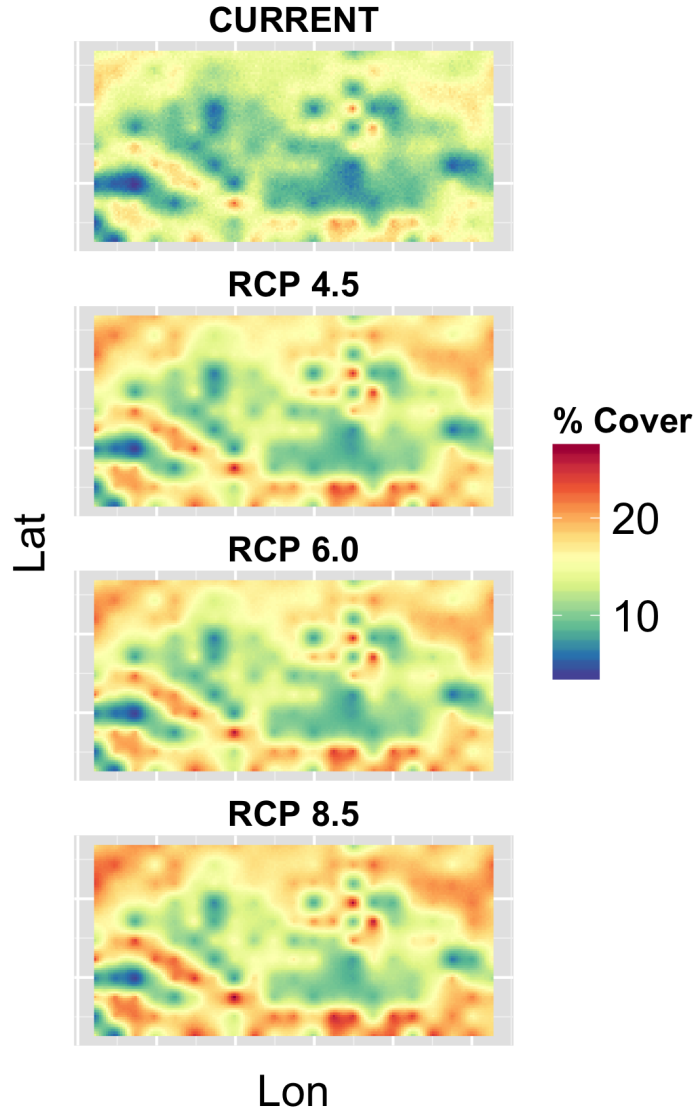
Figure 5: Projected equilibrium cover under three IPCC climate change scenarios (RCP = Representative Concentration Pathways) for our study area in southwestern Wyoming. The top panel shows equilibrium cover based on simulations using observed climate. Subsequent panels show equilibrium cover based on perturbed climate for each RCP scenario. Forecasts are based on the projected climate changes in Table 1 applied to the observed climate time series used to fit the statistical model. We used posterior mean parameter estimates for all simulations. Color bar indicates percent cover of sagebrush in each 30x30 meter pixel. Axes definitions: Lat = latitude; Lon = longitude.
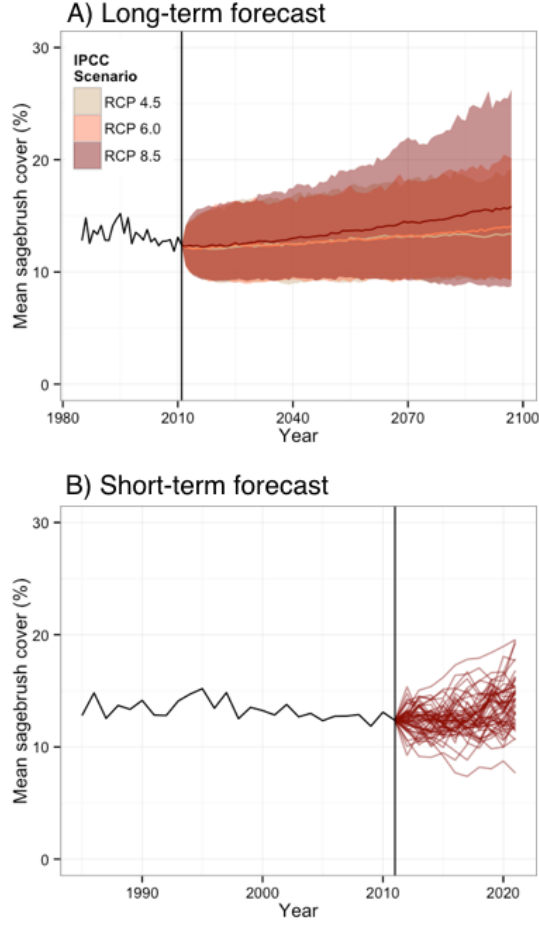
Figure 6: Observed (black line before 2011) and forecasted (colored lines after 2011) sagebrush percent cover. Long-term forecasts (A) were made for three IPCC emissions scenarios (RCPs 4.5, 6.0, and 8.5) and are for the period of 2012 to 2098. Shaded regions show limits of the 5th and 95th quantiles for simulations conducted using 50 different sets of parameters from the MCMC output. Lines show mean trajectories. Uncertainty in forecasts arises from uncertainty in GCM projections, uncerainty around the ecological process, and uncertainty around parameter estimates. Before calculating the mean and quantiles for each year across parameter sets and GCMs, we averaged percent cover over the 13,689 pixels. Panel (B) shows an example short-term forecast (10 years) using the MIROC5 GCM projections under RCP 8.5. Each line shows a forecast from one parameter set.

References

Adler, P. B., H. J. Dalgleish, and S. P. Ellner. 2012. Forecasting plant community impacts of climate variability and change: when do competitive interactions matter? Journal of Ecology 100:478–487.

Apodaca, L. F. 2013. Assessing Growth Response to Climate Controls in a Great Basin Artemisia Tridentata Plant Community. PhD thesis, University of Nevada Las Vegas.

Arnett, E. B., and T. Z. Riley. 2015. Science, policy, and the fate of the greater sage-grouse. Frontiers in Ecology and the Environment 13:235.

Baldeck, C. A., and G. P. Asner. 2014. Improving remote species identification through efficient training data collection. Remote Sensing 6:2682–2698.

Barry, R. P., and J. M. V. Hoef. 1996. Blackbox Kriging: Spatial Prediction without Specifying Variogram Models.

Bradford, J. B., and W. K. Lauenroth. 2006. Controls over invasion of Bromus tectorum: The importance of climate, soil, disturbance, and seed availability. Journal of Vegetation Science 17:693–704.

Bradley, B. A. 2010. Assessing ecosystem threats from global and regional change: hierarchical modeling of risk to sagebrush ecosystems from climate change, land use and invasive species in Nevada, USA. Ecography 33:198–208.

Bradshaw, G. A., and J. G. Borchers. 2000. Uncertainty as information: Narrowing the science-policy gap. Ecology and Society 4.

Clark, J. S., D. M. Bell, M. H. Hersh, and L. Nichols. 2011. Climate change vulnerability of forest biodiversity: Climate and competition tracking of demographic rates. Global Change Biology 17:1834–1849.

Clark, J. S., S. R. Carpenter, M. Barber, S. Collins, A. Dobson, J. A. Foley, D. M. Lodge, M. Pascual, R. Pielke, W. Pizer, C. Pringle, W. V. Reid, K. A. Rose, O. Sala, W. H.

Schlesinger, D. H. Wall, and D. Wear. 2001. Ecological forecasts: an emerging imperative. Science (New York, N.Y.) 293:657–660.

Clark, J. S., A. E. Gelfand, C. W. Woodall, and K. Zhu. 2014. More than the sum of the parts: Forest climate response from joint species distribution models. Ecological Applications 24:990–999.

Colgan, M. S., and G. P. Asner. 2014. Coexistence and environmental filtering of species-specific biomass in an African savanna. Ecology 95:1579–1590.

Conn, P. B., D. S. Johnson, J. M. V. Hoef, M. B. Hooten, J. M. London, and P. L. Boveng. 2015. Using spatiotemporal statistical models to estimate animal abundance and infer ecological dynamics from survey counts. Ecological Monographs 85:235–252.

Dalgleish, H. J., D. N. Koons, M. B. Hooten, C. A. Moffet, and P. B. Adler. 2011. Climate influences the demography of three dominant sagebrush steppe plants. Ecology 92:75–85.

Debinski, D. M., H. Wickham, K. Kindscher, J. C. Caruthers, and M. Germino. 2010. Montane meadow change during drought varies with background hydrologic regime and plant functional group. Ecology 91:1672–81.

Ehrlén, J., and W. F. Morris. 2015. Predicting changes in the distribution and abundance of species under environmental change. Ecology Letters 18:303–314.

Elith, J., and J. R. Leathwick. 2009. Species Distribution Models: Ecological Explanation and Prediction Across Space and Time.

Ellner, S. P., and M. Rees. 2006. Integral projection models for species with complex demography. The American naturalist 167:410–428.

Freckleton, R. P., W. J. Sutherland, A. R. Watkinson, and S. A. Queenborough. 2011. Density-structured models for plant population dynamics. American Naturalist 177:1–17.

Gelman, A., and J. Hill. 2009. Data analysis using regression and multilevel/hierarchical models. Cambridge University Press, Cambridge.

32

Gelman, A., and D. B. Rubin. 1992. Inference from Iterative Simulation Using Multiple Sequences. Statistical Science 7:457–472.

Gerber, B. D., W. L. Kendall, M. B. Hooten, J. A. Dubovsky, and R. C. Drewien. 2015. Optimal population prediction of sandhill crane recruitment based on climate-mediated habitat limitations. Journal of Animal Ecology 84:1299–1310.

Germino, M. J., and K. Reinhardt. 2014. Desert shrub responses to experimental modification of precipitation seasonality and soil depth: Relationship to the two-layer hypothesis and ecohydrological niche. Journal of Ecology 102:989–997.

Hare, J. a, M. a Alexander, M. J. Fogarty, E. H. Williams, and J. D. Scott. 2010. Forecasting the dynamics of a coastal fishery species using a coupled climate–population model. Ecological applications : a publication of the Ecological Society of America 20:452–464.

Harte, J., S. R. Saleska, and C. Levy. 2015. Convergent ecosystem responses to 23-year ambient and manipulated warming link advancing snowmelt and shrub encroachment to transient and long-term climate-soil carbon feedback. Global change biology 21:2349–56.

He, K. S., B. A. Bradley, A. F. Cord, D. Rocchini, M.-N. Tuanmu, S. Schmidtlein, W. Turner, M. Wegmann, and N. Pettorelli. 2015. Will remote sensing shape the next generation of species distribution models? Remote Sensing in Ecology and Conservation 1:4–18.

Higdon, D. 1998. A process-convolution approach to modelling temperatures in the North Atlantic Ocean. Environmental and Ecological Statistics 5:173–190.

Higdon, D. M. 2002. Space and space-time modeling using process convolutions. Pages 37–56 *in* C. Anderson, V. Barnett, P. Chatwin, and A. El-Shaarawi, editors. Quantitative methods for current environmental issues. Springer, London.

Hobbs, N. T., and M. B. Hooten. 2015. Bayesian Models: A Statistical Primer for Ecologists. Princeton University Press, Princeton.

Homer, C. G., C. L. Aldridge, D. K. Meyer, and S. J. Schell. 2012. Multi-scale remote

sensing sagebrush characterization with regression trees over Wyoming, USA: Laying a foundation for monitoring. International Journal of Applied Earth Observation and Geoinformation 14:233–244.

Homer, C. G., G. Xian, C. L. Aldridge, D. K. Meyer, T. R. Loveland, and M. S. O'Donnell. 2015. Forecasting sagebrush ecosystem components and greater sage-grouse habitat for 2050: Learning from past climate patterns and Landsat imagery to predict the future. Ecological Indicators 55:131–145.

Hooten, M. B., and N. T. Hobbs. 2015. A guide to Bayesian model selection for ecologists. Ecological Monographs 85:3–28.

Hooten, M. B., and C. K. Wikle. 2007. Shifts in the spatio-temporal growth dynamics of shortleaf pine. Environmental and Ecological Statistics 14:207–227.

Hooten, M. B., D. R. Larsen, and C. K. Wikle. 2003. Predicting the spatial distribution of ground flora on large domains using a hierarchical Bayesian model. Landscape Ecology 18:487–502.

Kuchler, A. 1964. Potential Natural Vegetation of the Conterminous United States. American Geographical Society, Special Publication No. 36.

Latimer, A. M., S. Banerjee, H. Sang, E. S. Mosher, and J. A. Silander. 2009. Hierarchical models facilitate spatial analysis of large data sets: A case study on invasive plant species in the northeastern United States. Ecology Letters 12:144–154.

Luo, Y., K. Ogle, C. Tucker, S. Fei, C. Gao, S. LaDeau, J. S. Clark, and D. S. Schimel. 2011. Ecological forecasting and data assimilation in a data-rich era. Ecological Applications 21:1429–1442.

Maiorano, L., R. Cheddadi, N. E. Zimmermann, L. Pellissier, B. Petitpierre, J. Pottier, H. Laborde, B. I. Hurdu, P. B. Pearman, A. Psomas, J. S. Singarayer, O. Broennimann, P. Vittoz, A. Dubuis, M. E. Edwards, H. A. Binney, and A. Guisan. 2013. Building the niche

34

through time: using 13,000 years of data to predict the effects of climate change on three tree species in Europe. Global Ecology and Biogeography 22:302–317.

Merow, C., A. M. Latimer, A. M. Wilson, S. M. McMahon, A. G. Rebelo, and J. A. Silander. 2014. On using integral projection models to generate demographically driven predictions of species' distributions: development and validation using sparse data. Ecography 37:1167–1183.

Miglia, K., E. Mcarthur, W. Moore, H. Wang, J. Graham, and D. Freeman. 2005. Nine-year reciprocal transplant experiment in the gardens of the basin and mountain big sagebrush (Artemisia tridentata: Asteraceae) hybrid zone of Salt Creek Canyon: the importance of multiple-year tracking of fitness Title. Biological Journal of the Linnean Society:213–225.

Neilson, R., J. Lenihan, D. Bachelet, and R. Drapek. 2005. Climate change implications for sagebrush ecosystems. Page 145 *in* North american wildlife and natural resources conference.

Pechanec, J., G. Pickford, and G. Stewart. 1937. Effects of the 1934 Drought on Native Vegetation of the Upper Snake River Plans, Idaho. Ecology:490–505.

Perfors, T., J. Harte, and S. E. Alter. 2003. Enhanced growth of sagebrush (Artemisia tridentata) in response to manipulated ecosystem warming. Global Change Biology 9:736–742.

Petchey, O. L., M. Pontarp, T. M. Massie, S. Kéfi, A. Ozgul, M. Weilenmann, G. M. Palamara, F. Altermatt, B. Matthews, J. M. Levine, D. Z. Childs, B. J. McGill, M. E. Schaepman, B. Schmid, P. Spaak, A. P. Beckerman, F. Pennekamp, and I. S. Pearse. 2015. The ecological forecast horizon, and examples of its uses and determinants. Ecology Letters 18:597–611.

Poore, R. E., C. A. Lamanna, J. J. Ebersole, and B. J. Enquist. 2009. Controls on Radial Growth of Mountain Big Sagebrush and Implications for Climate Change. Western North

American Naturalist 69:556–562.

Queenborough, S. A., K. M. Burnet, W. J. Sutherland, A. R. Watkinson, and R. P. Freckleton. 2011. From meso- to macroscale population dynamics: A new density-structured approach. Methods in Ecology and Evolution 2:289–302.

R Core Team. 2013. R: A language and environment for statistical computing.

Rees, M., and S. P. Ellner. 2009. Integral projection models for populations in temporally varying environments. Ecological Monographs 79:575–594.

Roberts, D. R., and A. Hamann. 2012. Predicting potential climate change impacts with bioclimate envelope models: A palaeoecological perspective. Global Ecology and Biogeography 21:121–133.

Ross, B. E., M. B. Hooten, J.-M. DeVink, and D. N. Koons. 2015. Combined effects of climate, predation, and density dependence on Greater and Lesser Scaup population dynamics. Ecological Applications 25:1606–1617.

Running, S. W., R. R. Nemani, F. A. Heinsch, M. Zhao, M. Reeves, and H. Hashimoto. 2004. A Continuous Satellite-Derived Measure of Global Terrestrial Primary Production. BioScience 54:547.

Rupp, D. E., J. T. Abatzoglou, K. C. Hegewisch, and P. W. Mote. 2013. Evaluation of CMIP5 20th century climate simulations for the Pacific Northwest US. Journal of Geophysical Research 118:1–23.

Salguero-Gómez, R., O. R. Jones, C. R. Archer, Y. M. Buckley, J. Che-Castaldo, H. Caswell, D. Hodgson, A. Scheuerlein, D. A. Conde, E. Brinks, H. de Buhr, C. Farack, F. Gottschalk, A. Hartmann, A. Henning, G. Hoppe, G. Römer, J. Runge, T. Ruoff, J. Wille, S. Zeh, R. Davison, D. Vieregg, A. Baudisch, R. Altwegg, F. Colchero, M. Dong, H. de Kroon, J.-D. Lebreton, C. J. E. Metcalf, M. M. Neel, I. M. Parker, T. Takada, T. Valverde, L. A. Vélez-Espino, G. M. Wardle, M. Franco, and J. W. Vaupel. 2015. The

compadrePlant Matrix Database: an open online repository for plant demography. Journal of Ecology 103:202–218.

Schlaepfer, D. R., W. K. Lauenroth, and J. B. Bradford. 2011. Ecohydrological niche of sagebrush ecosystems. Ecohydrology:n/a–n/a.

Schlaepfer, D. R., W. K. Lauenroth, and J. B. Bradford. 2014a. Modeling regeneration responses of big sagebrush (Artemisia tridentata) to abiotic conditions. Ecological Modelling 286:66–77.

Schlaepfer, D., W. K. Lauenroth, and J. B. Bradford. 2014b. Natural Regeneration Processes in Big Sagebrush (Artemisia tridentata). Rangeland Ecology & Management 67:344–357.

Schlaepfler, D., W. K. Lauenroth, and J. B. Bradford. 2012. Effects of ecohydrological variables on current and future ranges, local suitability patterns, and model accuracy in big sagebrush. Ecography 5:453–466.

Schurr, F. M., J. Pagel, J. S. Cabral, J. Groeneveld, O. Bykova, R. B. O'Hara, F. Hartig, W. D. Kissling, H. P. Linder, G. F. Midgley, B. Schröder, A. Singer, and N. E. Zimmermann. 2012. How to understand species' niches and range dynamics: A demographic research agenda for biogeography. Journal of Biogeography 39:2146–2162.

Shafer, S. L., P. J. Bartlein, and R. S. Thompson. 2001. Potential changes in the distributions of western North America tree and shrub taxa under future climate scenarios. Ecosystems 4:200–215.

Shriver, R. K. 2015. Quantifying how short-term environmental variation leads to long-term demographic responses to climate change. Journal of Ecology:n/a–n/a.

Stan Development Team. 2014a. Stan: A C++ Library for Probability and Sampling, Version 2.5.0.

Stan Development Team. 2014b. Rstan: the R interface to Stan, Version 2.5.0.

Still, S., and B. Richardson. 2015. Projections of Contemporary and Future Climate Niche for Wyoming Big Sagebrush (Artemisia tridentata subsp. wyomingensis): A Guide for Restoration. Natural Areas Journal 35:30–43.

Vanderwel, M. C., V. S. Lyutsarev, and D. W. Purves. 2013. Climate-related variation in mortality and recruitment determine regional forest-type distributions. Global Ecology and Biogeography 22:1192–1203.

Wikle, C. K. 2010. Low-rank representations for spatial processes. Pages 89–106 *in* A. Gelfand, P. Diggle, M. Fuentes, and P. Guttopr, editors. Handbook of spatial statistics. Chapman; Hill, Upper Saddle River, New Jersey, USA.

Xian, G., C. G. Homer, and C. L. Aldridge. 2012. Effects of Land Cover and Regional Climate Variations on Long-Term Spatiotemporal Changes in Sagebrush Ecosystems. GI-Science & Remote Sensing 49:378–396.